Electronic Supplementary Material (ESI) for Chemical Communications.

Supporting Information

Time gated Fourier transform spectroscopy with burst excitation for time-resolved spectral maps from the nano- to millisecond range

Mikkel Baldtzer Liisberg[a,*] Vanessa Rück,[a] and Tom Vosch[a,*]

[a]Nanoscience Center and Department of Chemistry, University of Copenhagen, Universitetsparken 5, 2100 Copenhagen, Denmark. Email: mbl@chem.ku.dk; tom@chem.ku.dk

Supplementary Note 1: Experimental Setup.

The experimental setup used for bmTG-FTS is an extension of our TG-FTS[1] implementation with the addition of a device for adjusting the profile of the excitation source to appear in bursts of variable durations.

The measurements were carried out on a home-built microscope setup. A fiber coupled (FD7-PM, NKT Photonics) continuum white-light laser (SuperK EXTREME EXB-6, NKT Photonics) with a repetition rate of 13 MHz was used as an excitation source delivering a wavelength of 520 nm by sending the continuum output through an acousto-optic tunable filter (SuperK SELECT, NKT Photonics). The excitation light was cleaned up with a 520 nm band-pass filter (Semrock, FF01-520/5-25) before being expanded (BE05M-A, Thorlabs). The excitation light was then reflected by a 30:70 beam splitter (XF122, Omega Optical) and sent through an oil immersion objective (UPlanSAPO 100x NA = 1.3, Olympus), which focused the laser onto the sample. Luminescence was collected from the same objective, and residual excitation light was removed with a 532 nm long-pass filter (BLP01-532-25, Semrock). The emission light was directed through the TWINS device (GEMINI, NIREOS) and finally detected on an avalanche photodiode (APD; SPCM-AQRH-14-TR, Excelitas Technologies) connected to a single photon counting module (SPC-830, Becker & Hickl). Count rates were adjusted to be significantly below the repetition rate in order to avoid pile-up effects.

The burst profile of the excitation source is controlled by driving the AOTF crystal with a variable external signal. The AOTF crystal is connected to an external radio frequency (RF) driver; this RF driver is in turn connected to a separate module (SuperK COMMAND, NKT Photonics) that is able to drive and synchronize fast wavelength switching or amplitude modulation of the output of the AOTF based on input from an external source. As an external source, we used a delay generator (DG535, Stanford Research Systems) with an internal trigger (f_{Macro} = 1 kHz). This allowed us to prepare bursts with variable on and off periods; for all measurements presented here, we had T_{on} = 0.4 ms and T_{off} = 0.6 ms. A 5 ns TTL pulse from a second port of the same delay generator was sent to the multichannel router of the TCSPC board, marking the beginning of each burst. More details on the generation of burst profiles can be found in Liisberg et al.[2]

Supplementary Note 2: Data Collection.

All data was collected using LabVIEW, while all subsequent data analysis was performed with self-written MATLAB routines. Official VIs from NIREOS and Becker & Hickl were modified and combined to allow for collecting TRIMs. There are two major differences between our last implementation (TG-FTS)[1] and bmTG-FTS. Firstly, in TG-FTS, we only consider the micro-time domain, while we in bmTG-FTS consider both the micro- and macro-time domains. Accordingly, we collect first-in-first-out (FIFO) files at each position of the interferometer rather than merely a single micro-time decay. The FIFO files contain both the micro- and macro-times of each collected photon along with the channel number (0 for APD signal and 1 for burst-sync). Secondly, we use a burst-mode excitation scheme to allow for assessing the dynamics of long-lived emitters/states. Thus, at each position of the interferometer, multiple on/off cycles are recorded to ensure significant counts, and the burst-sync is used to subsequently overlay the recorded cycles. With an integration time of 10 s at each position and f_{Macro} = 1 kHz, approximately 10,000 cycles are collected per position.

For the measurements of $(DNA)_2[Ag_{18}]^{12+}$, we scanned a total range of 0.7 mm in 350 steps, while we for the IRF scanned a range of 4 mm in 2000 steps (note that we only used an integration time of 0.1 s per position for the IRF rather than 10 s).

Supplementary Note 3: Data Analysis.

The data analysis conducted in bmTG-FTS is in many regards similar to the data analysis of TG-FTS. In fact, for the analysis of all micro-time related data (i.e., the preparation of ungated and time gated mTRIM/mTREM), we use the same framework developed in TG-FTS. Accordingly, we refer to the SI of Liisberg et al,[1] where we have given a detailed description of how the micro-time related data is analyzed. Here, we instead focus our attention on the analysis of the macro-time aspect of the data and how gating in the micro-time domain can be used to prepare MTRIMs and MTREMs that are either fluorescence or luminescence gated.

First, we consider the case of how the data is analyzed in an ungated approach (Fig. S8). As an initial step, we import the raw FIFO files that were generated during data collection (Fig. S8a). A FIFO file is imported for each displacement, x, of the interferometer. These files contain the macro- (T) and micro-times (t) along with the channel number (Ch.) of all photons collected during the

10 s long acquisition (see, for instance, the first and last couple of photons collected at -0.35 mm and 0.35 mm shown in the tables of Fig. S8a). The histograms of the macro-times (bottom graphs in Fig. S8a) clearly show the individual bursts that occur every 1 ms with the burst sync signals precisely marking the beginning of each burst. Subsequently, we overlap all the bursts for each displacement (Fig. S8b); accordingly, the histograms (bottom graphs) only show a single on/off cycle. For this step, we used the methodology developed by Liisberg et al.[2] By preparing a histogram (considering both the micro- and macro-times) at every displacement, we are able to prepare the mTRIM and MTRIM (Fig. S8c). The mTRIM and MTRIM are then position calibrated with an official LABVIEW VI from NIREOS (Fig. S8d); note that this is the only data analysis step not performed in MATLAB. Finally, to obtain the mTREM and MTREM, we perform a FT along the displacement axis followed by a wavelength and intensity calibration (Fig. S8e). See Perri et al.[3] and Liisberg et al.[1] for more details on the wavelength and intensity calibration, respectively.

To prepare fluorescence or luminescence gated MTRIMs, we start from having the macro-times overlapped at each displacement (Fig. S9a, similar to Fig. S8b). Based on the fluorescence decay in the micro-time domain, a suitable micro-time window is decided upon; in this case, we use a fluorescence window from 41 ns to 55 ns. Accordingly, each photon is assigned as either a fluorescence or luminescence photon, based on whether the micro-time is inside or outside the defined time gate (Fig. S9a, red or blue color-coded photons are fluorescence or luminescence, respectively). The histograms (bottom graphs) of the fluorescence and luminescence gated macro-times now clearly reveal how the two contributions have been disentangled from one another. Note that we correct for residual luminescence within the fluorescence window, as described in Liisberg et al.[1] From this point, the analysis is the same as for the ungated case, but now instead performed for the fluorescence and luminescence gated photons. Thus, we prepare a histogram at every displacement for both the fluorescence and luminescence gated photons (Fig. S9b) and subsequently position calibrate the MTRIMs (Fig. S9c). Then, for the preparation of the MTREMs, we perform a FT along the displacement axis of the MTRIMs followed by a wavelength and intensity calibration (Fig. S9d).

The code used in this paper is available at https://doi.org/10.17894/ucph.0d48d2d7-18a9-474a-b59d-37b1638ba62d.

Additional Figures.

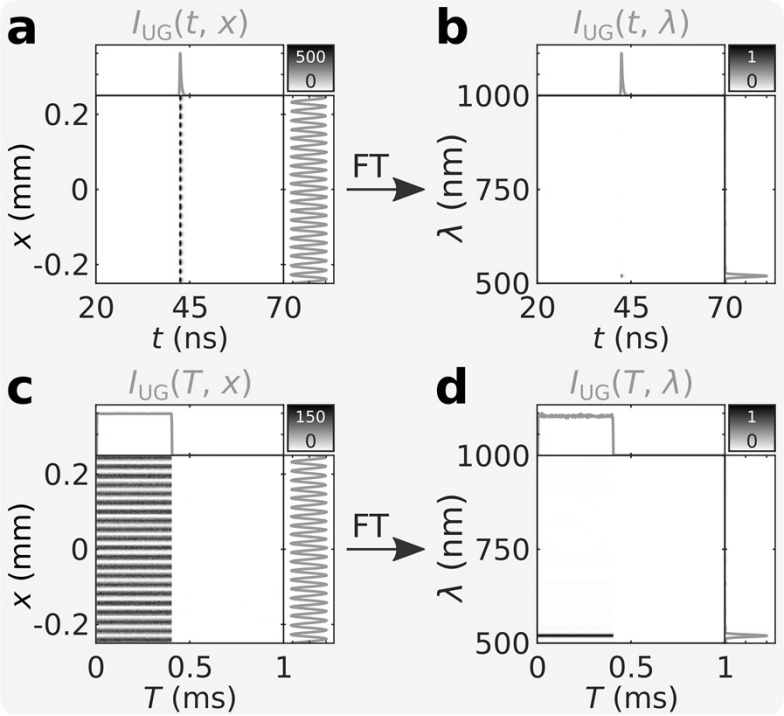

Fig. S1 Ungated bmFTS data of instrument response function (λ_{Ex} = 520 nm, f_{Micro} = 13 MHz, f_{Macro} = 1 kHz, T_{on} = 0.4 ms, T_{off} = 0.6 ms). Micro-time domain (a) TRIM and (b) TREM. Macro-time domain TRIM (c) and TREM (d).

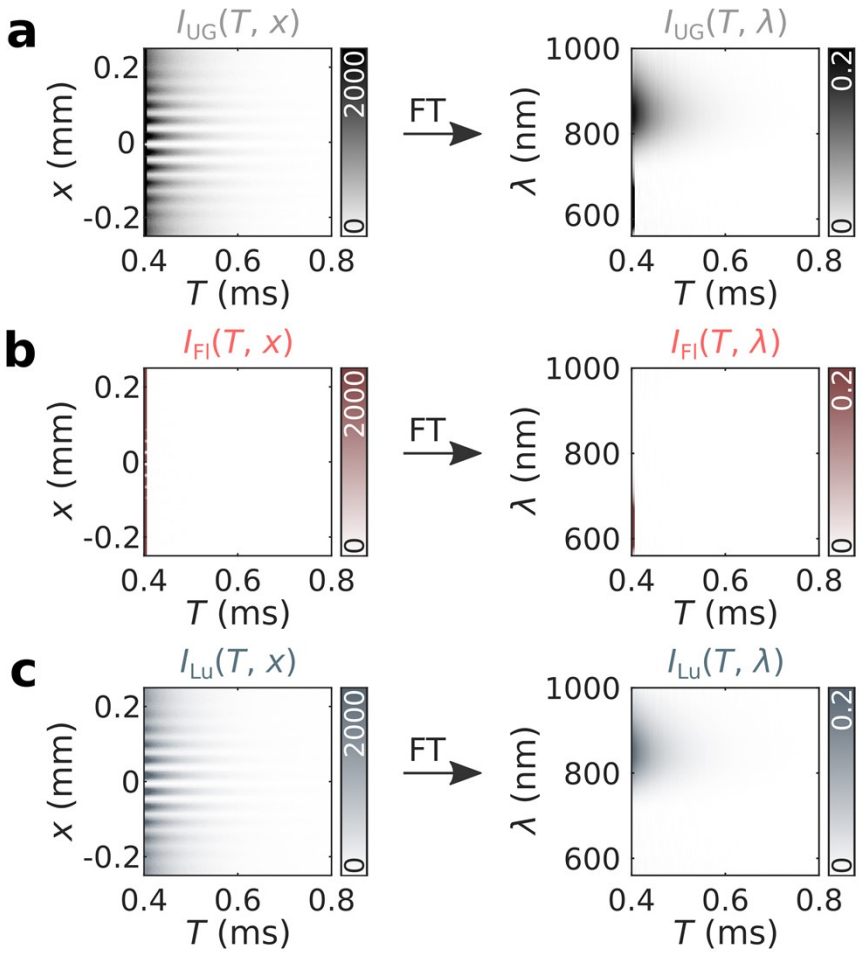

Fig. S2 Close-ups of MTRIMs and MTREMs during the off period of the burst cycle. The data is from an aqueous solution of $(DNA)_2[Ag_{18}]^{12+}$ at RT excited at 520 nm (I = 3.4 kW/cm^2, f_{Micro} = 13 MHz, f_{Macro} = 1 kHz, T_{on} = 0.4 ms, T_{off} = 0.6 ms). (a) Ungated, (b) fluorescence gated, and (c) luminescence gated MTRIMs (left) and MTREMs (right).

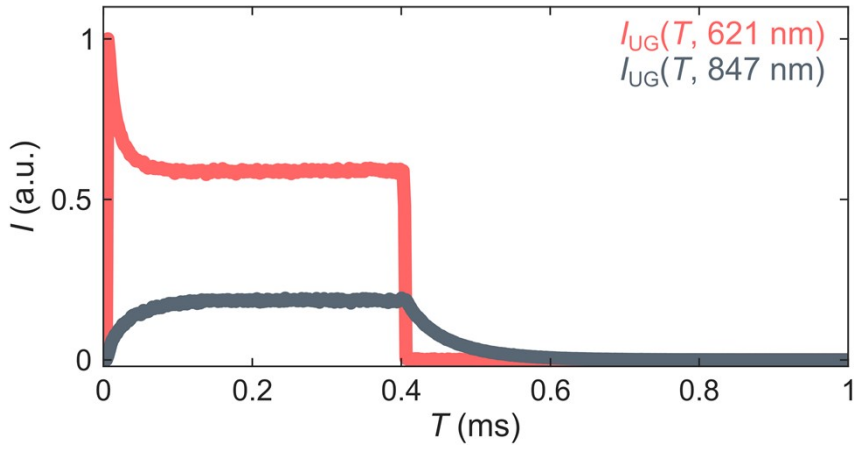

Fig. S3 Intensity responses from the ungated MTREM ($I_{UG}(T, \lambda)$) at the maxima of the two bands, as indicated by the dashed lines in Fig. 2.

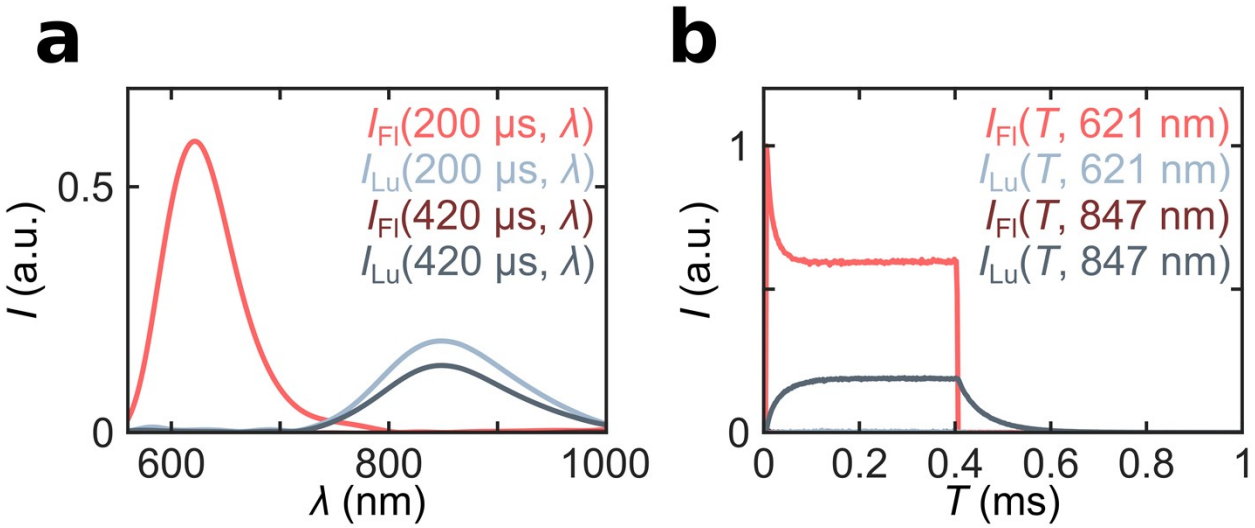

Fig. S4 Time-resolved emission spectra and intensity responses from the gated TREMs $I_{Fl}(T, \lambda)$ and $I_{Lu}(T, \lambda)$. (a) Spectra of the fluorescence and luminescence at 200 µs and 420 µs from the start of the burst. (b) Evolution of the fluorescence (621 nm) and luminescence (847 nm) response during the burst cycle.

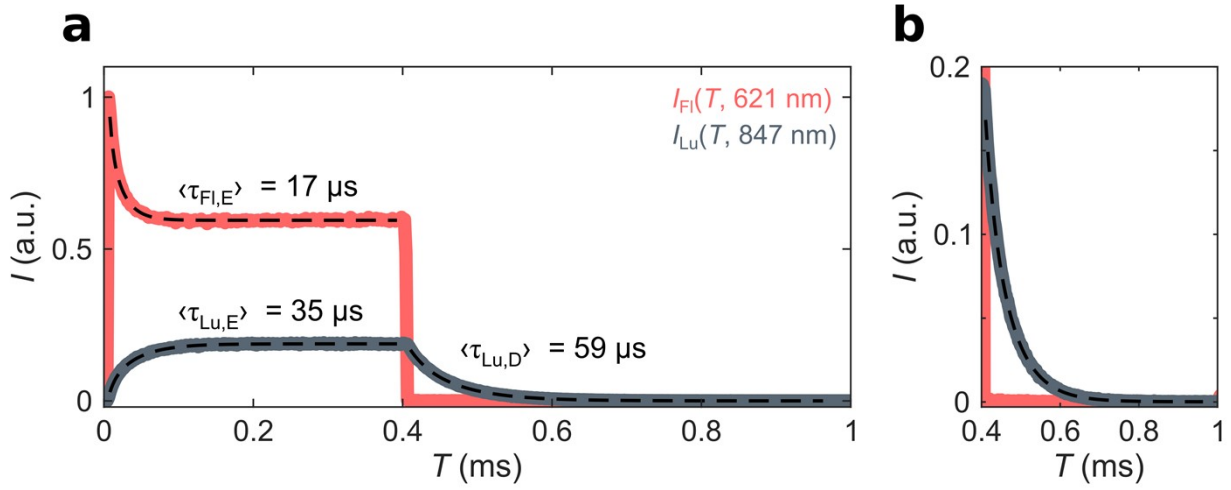

Fig. S5 Bi-exponentially tail-fitted equilibrium and decay times of traces shown in Fig. S4b. (a) Full burst cycle showing the equilibration of the fluorescent and luminescent states during the on period of the burst, and the decay of the luminescent state during the off period of the burst. (b) A close-up view of the luminescence decay during the off period of the burst.

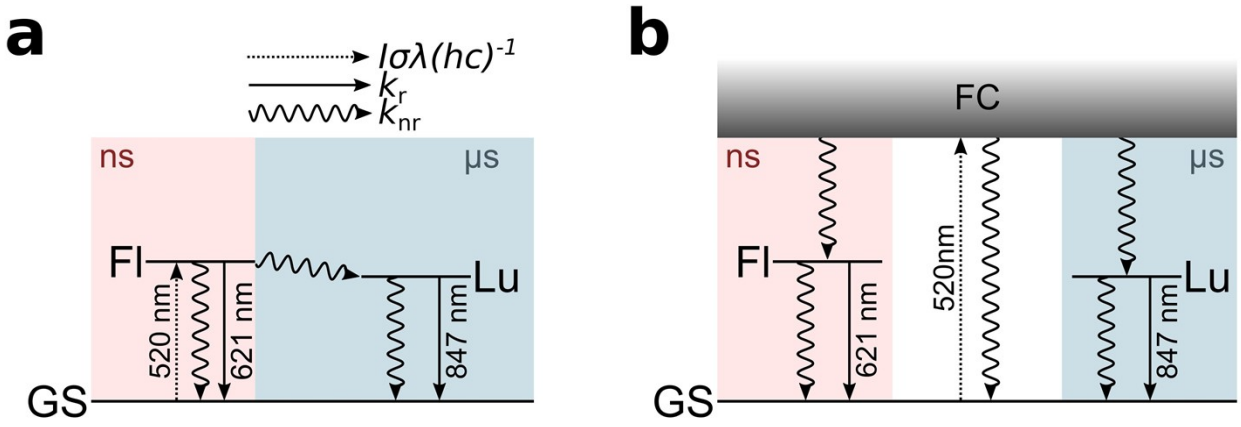

Fig. S6 Energy diagrams of a (a) three-level and (b) four-level model. In the three-level model, excitation proceeds directly through the fluorescent (Fl) state. The long-lived state (Lu) is thus populated from the Fl state, which necessitates that the equilibration time of Lu ($\tau_{Lu,E}$) equals that of Fl ($\tau_{Fl,E}$). In the four-level model, excitation instead proceeds through a short-lived Franck-Condon state (FC), from which both Fl and Lu are populated. Contrary to the three-level model, the equilibration rates of Fl and Lu are not directly coupled and may thus take different values, as is observed for $(DNA)_2[Ag_{18}]^{12+}$. Previously, other DNA-AgNCs have been observed to follow both three-level[4] and four-level[5, 6] models. Note that the energy diagrams are schematic, and that the energy Y-axis is not absolute in nature.

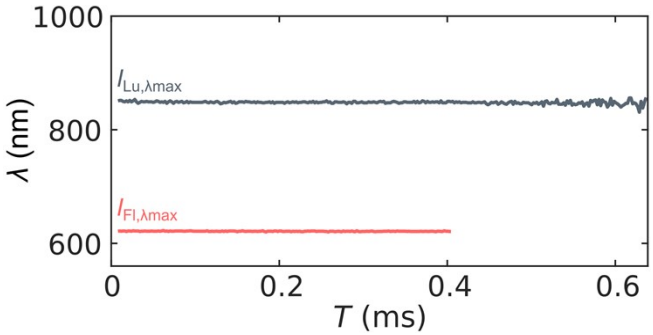

Fig. S7 Wavelength maxima of fluorescence ($I_{Fl,\lambda max}$) and luminescence ($I_{Lu,\lambda max}$) gated MTREMs as a function of time during the on/off period of the burst, shown here for the data presented in Fig. 3.

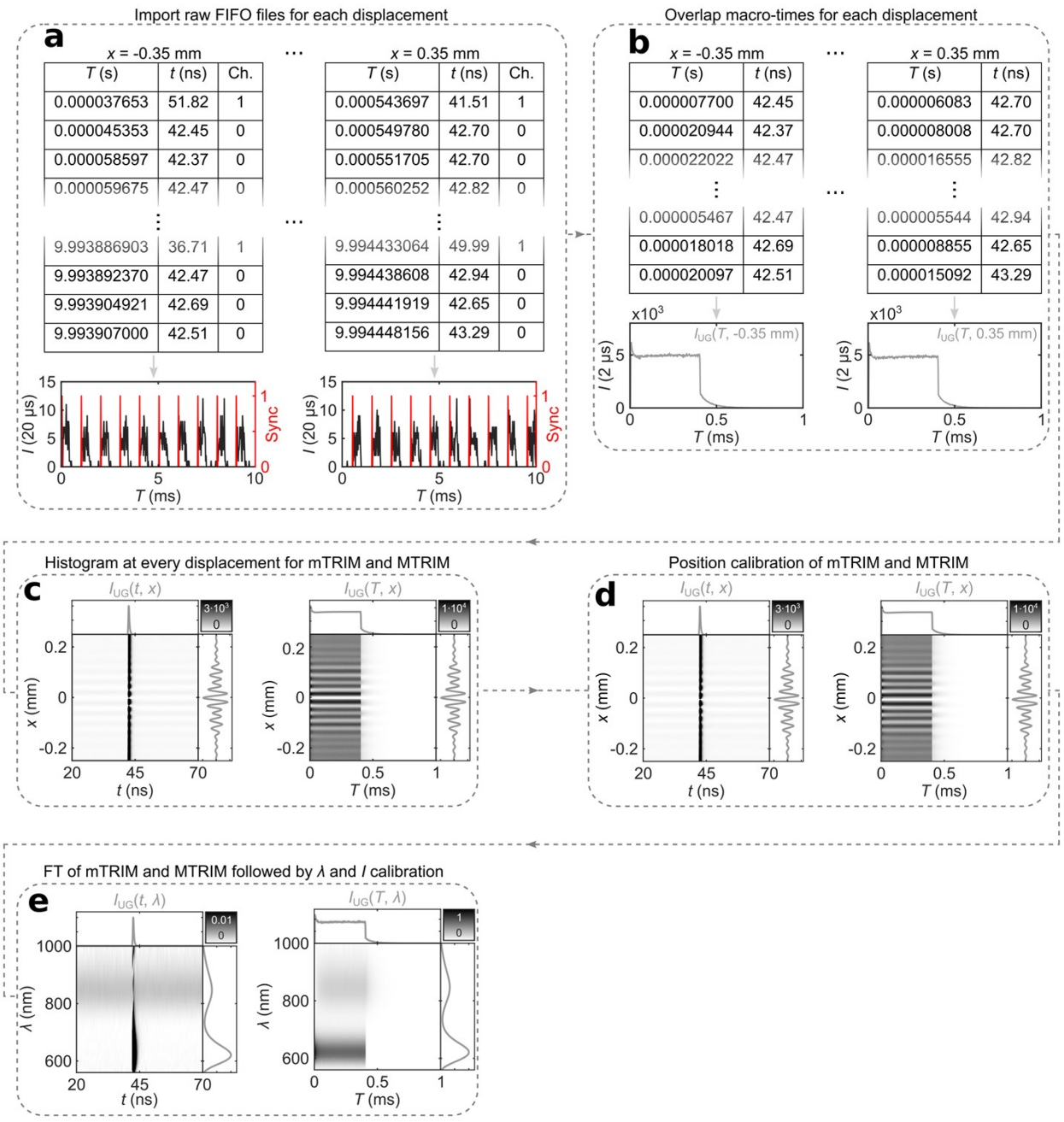

Fig. S8 Overview of steps involved in the analysis of bmFTS data for the preparation of an ungated mTREM and MTREM. (a) The raw FIFO files for each displacement are imported, which contain the macro- (T) and micro-time (t) along with channel number (Ch., 0 for fluorescence/luminescence signal and 1 for burst sync signal) of each detected photon. The bottom graphs show the histograms of the macro-times of fluorescence/luminescence (black) and sync (red). (b) Each burst is overlapped for every displacement. (c) The mTRIM and MTRIM are produced by preparing a histogram of the micro- and macro-times at every displacement. (d) The

mTRIM and MTRIM are position calibrated. (e) The mTREM and MTREM are finally obtained by performing a FT along the displacement axis followed by a wavelength and intensity calibration.

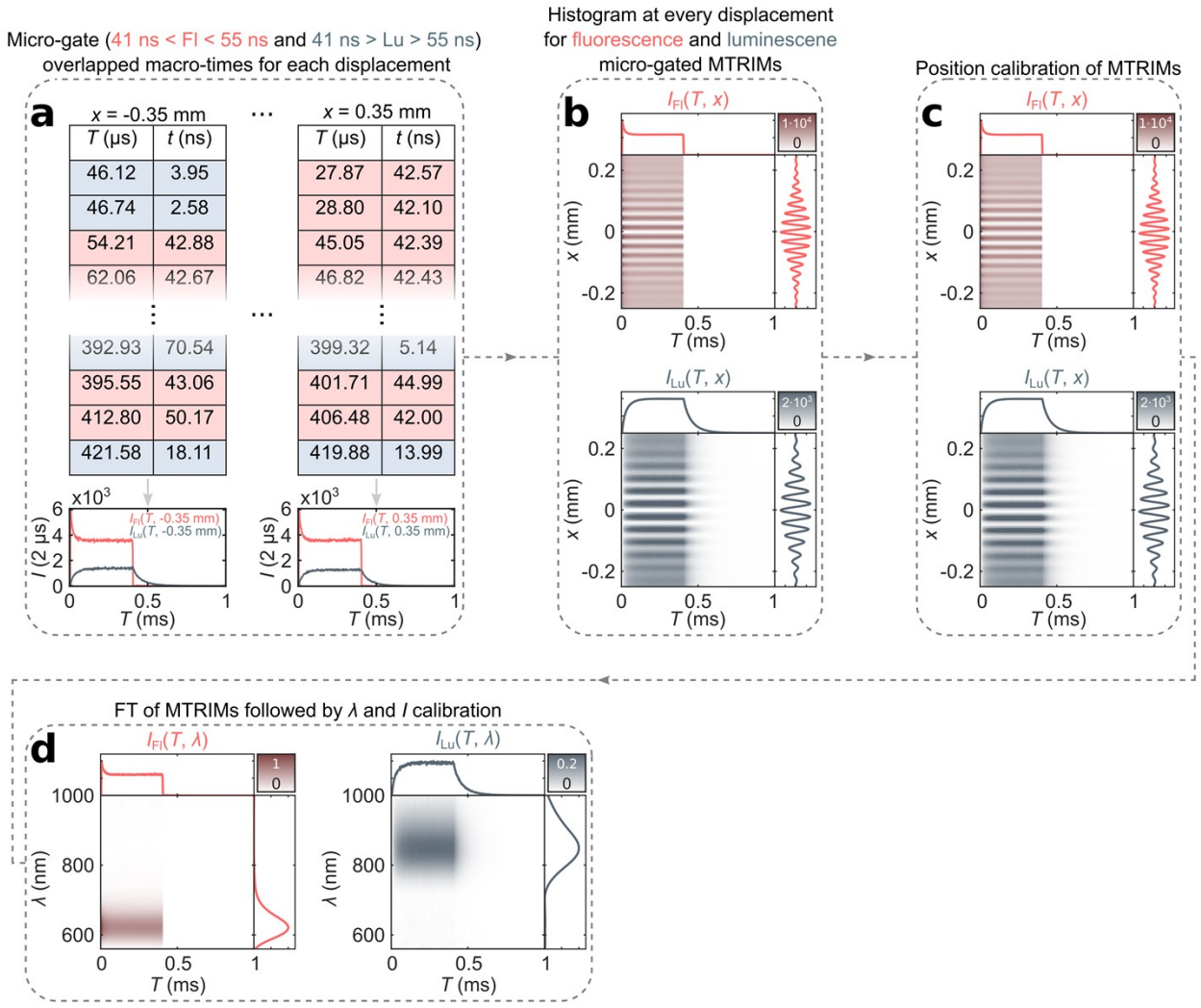

Fig. S9 Overview of steps involved in the preparation of fluorescence and luminescence gated MTREMs. (a) The overlapped macro-times for each displacement (similar to Fig. S8b) are micro-gated based on whether they appear in the fluorescence (within 41 ns – 55 ns, colored red) or luminescence (outside 41 ns – 55 ns, colored blue) micro-time window. The bottom graphs show the histograms of the macro-times of the fluorescence (red) and luminescence (blue) gated photons. (b) The fluorescence and luminescence gated MTRIMs are produced by preparing a histogram of the macro-times at every displacement. (d) The MTRIMs are position calibrated.

(e) The MTREMs are finally obtained by performing a FT along the displacement axis followed by a wavelength and intensity calibration.

References.

1 M. B. Liisberg and T. Vosch, *Commun. Mater.* **2023**, *4*, 57.
2 M. B. Liisberg, S. Krause, C. Cerretani and T. Vosch, *Chem. Sci.* **2022**, *13*, 5582-5587.
3 A. Perri, *J. Phys. B: At. Mol. Opt. Phys.* **2021**, *54*, 113001.
4 J. T. Petty, S. Carnahan, D. Kim and D. Lewis, *J. Chem. Phys.* **2021**, *154*, 244302.
5 S. Krause, M. R. Carro-Temboury, C. Cerretani and T. Vosch, *PCCP* **2018**, *20*, 16316-16319.
6 S. A. Patel, M. Cozzuol, J. M. Hales, C. I. Richards, M. Sartin, J.-C. Hsiang, T. Vosch, J. W. Perry and R. M. Dickson, *J. Phys. Chem. C* **2009**, *113*, 20264-20270.